Moscow Institute of Physics and Technology
(State University)
Landau Institute for Theoretical Physics, RAS

Bachelor's thesis

Magnetoconductance of a $p-n$ junction in a Weyl semimetal

Author:
322nd group student — David R. Saykin

Supervisor:
Cand. Sci. (Phys.-Math.) — Konstantin S. Tikhonov

Moscow, 30 June 2017

Abstract

Dear reader, I welcome you to the pages of my thesis, and I want to warn you that this manuscript was written in the hope of being read, and therefore does not conform to the general template of theses. I believe that the only interested reader, apart, perhaps, from the reviewer, can only be a physics student who is just beginning to study theoretical physics, but by no means a seasoned theoretical scientist who, in the line of duty, devours a dozen scientific articles before breakfast. For this reason, I try to present the material in a consistent and comprehensible manner. As a result, the text of the first chapter and of the appendices is of a pedagogical rather than a scientific character.

Before proceeding to the presentation of the main material, I introduce the reader to a relatively new class of topological materials — the Weyl semimetal — in chapter 1 I describe the ways of theoretically describing such materials and their experimental discovery.

A reader interested only in the results that claim scientific novelty should turn directly to chapter 2, in which I proceed to describe the solution of the main problem of this work — the study of the conductance of a ballistic $p{-}n$ junction in a T–symmetric Weyl semimetal (of the TaAs type) as a function of the magnetic field.

The consideration of the problem is based on the work [1], in which the magneto-conductance G was computed in a model with the Hamiltonian

$$\hat{H} = v\boldsymbol{\sigma} \cdot \mathbf{p}.$$

The main results of the article [1] are analyzed in appendix B. I, in turn, consider the Hamiltonian describing a pair of Weyl nodes [2],

$$\hat{H} = \frac{\sigma_x}{2m}(p_x^2 - p_0^2) + v\sigma_y p_y + v\sigma_z p_z,$$

and I find a sign change of the differential conductance dG/dB at fields of the order of $B_0 \sim \Phi_0 k_0^2$, where k_0 is the distance between the Weyl nodes, and Φ_0 is the magnetic flux quantum.

Contents

Chapter 1

Weyl semimetal

1.1 Dirac or Weyl?

The Dirac and Weyl equations

In 1928 Paul Dirac wrote down the quantum equation of motion for relativistic electrons, i. e. particles with spin $s = \frac{1}{2}$.

$$i\partial_t \Psi = \left[c\boldsymbol{\alpha}\hat{\mathbf{p}} + \beta mc^2\right]\Psi, \quad \varepsilon(\mathbf{p}) = \pm\sqrt{c^2p^2 + m^2c^4}. \tag{1.1}$$

where the Hermitian matrices α^i, β are defined by the anticommutation relations

$$\{\alpha^i, \alpha^j\} = 2\delta^{ij}, \quad \{\alpha^i, \beta\} = 0, \quad \beta^2 = 1. \tag{1.2}$$

Shortly afterwards, in 1929, Hermann Weyl considered the case $m = 0$ and noticed that in the representation $\boldsymbol{\alpha} = \boldsymbol{\sigma} \otimes \sigma^z$ the matrix $\hat{\chi} = \hat{\mathbb{1}} \otimes \sigma^z$ commutes with the Hamiltonian.[1] He proposed to look for solutions of (1.1) within its eigensubspaces. This quantum number is customarily called the chirality $\chi = \pm$, and the corresponding eigenfunctions the right and left spinors.

$$\begin{aligned} i\partial_t\psi &= +c\boldsymbol{\sigma}\hat{\mathbf{p}}\psi \\ i\partial_t\phi &= -c\boldsymbol{\sigma}\hat{\mathbf{p}}\phi \end{aligned} \qquad \Psi = \begin{pmatrix}\psi \\ \phi\end{pmatrix} \qquad \varepsilon(\mathbf{p}) = \pm c|\mathbf{p}|. \tag{1.3}$$

The system (1.3) describes a *massless Dirac fermion* Ψ, while each of the equations (1.3) taken separately is called the Weyl equation (of definite chirality) and describes *Weyl fermions* ψ, ϕ.

Weyl spinors were used to describe neutrinos [3, §30], until it became known that they have a finite mass. To date, physics knows of no examples of Weyl particles; however, electrons in a solid can have a dispersion that is described by the Dirac and Weyl equations.

The simplest example of a host for a Dirac electron is graphene — a two-dimensional monolayer of graphite, discovered experimentally in 2005. Low-energy excitations in graphene are described by the Hamiltonian

$$\mathcal{H}(\mathbf{p}) = v\sigma_x p_x + v\sigma_y p_y, \quad \varepsilon(\mathbf{p}) = \pm v|\mathbf{p}|, \tag{1.4}$$

which is customarily called (massless) Dirac rather than Weyl when one deals with a two-dimensional system. In dimension $2 + 1$ the Clifford algebra (1.2) has a simple

[1] Such a matrix can be constructed in any space of odd dimension as $\gamma^5 = -i\alpha^1\alpha^2\alpha^3$.

representation in terms of the Pauli matrices $\alpha_1 = \sigma_1$, $\alpha_2 = \sigma_2$, $\beta = \sigma_3$, so that equation (1.1) can be rewritten as

$$i\partial_t \Psi = \left[c\sigma_x \hat{p}_x + c\sigma_y \hat{p}_y + \sigma_z mc^2\right] \Psi, \tag{1.5}$$

and the Dirac fermion is described by a two-component spinor Ψ. One can see how such quasiparticles arise in graphene by considering the tight-binding model.

Thus three-dimensional Weyl fermions are analogues of the two-dimensional massless Dirac particles in graphene. However, Weyl quasiparticles have a number of properties that differ from those of electrons in graphene. For example, the presence of Fermi arcs — surface states that lead to unusual oscillations of the density of states with magnetic field [4].

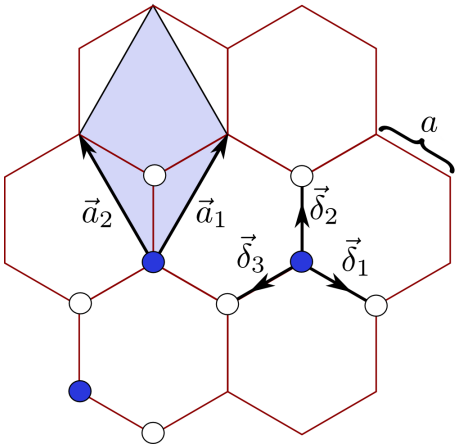

(a) Graphene lattice, elementary translation vectors $\mathbf{a}_i$, nearest-neighbor vectors $\boldsymbol{\delta}_j$.

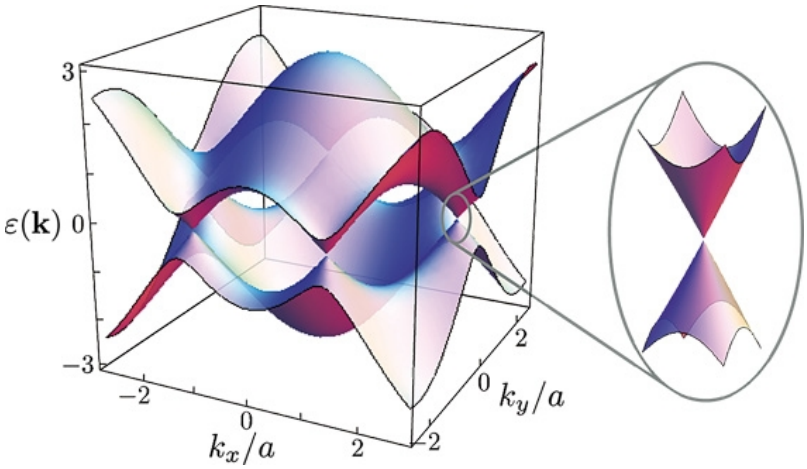

(b) Graphene spectrum in the tight-binding approximation (Fermi level at $\varepsilon = 0$). Near the points $\mathbf{k} = (\pm\frac{4\pi}{3\sqrt{3}a}, 0)$ the excitations take the form of a Weyl cone.

Figure 1.1: Crystal lattice of graphene and the spectrum of electronic excitations.

Graphene in the tight-binding approximation

In the simplest approximation, which takes into account only nearest-neighbor hopping, the Hamiltonian of electrons in graphene is

$$\hat{H} = t \sum_{\langle i,j \rangle} \hat{c}^+(\mathbf{r}_i)\hat{c}(\mathbf{r}_j) = t \sum_{\mathbf{r}}^{\mathrm{SL}} \sum_{j=1}^{3} \hat{c}_A^+(\mathbf{r})\hat{c}_B(\mathbf{r} + \boldsymbol{\delta}_j) + \text{h.c.}, \tag{1.6}$$

where the summation runs over nearest neighbors. The crystal lattice (see Fig. 1.1a) of graphene consists of two triangular sublattices, with translation vectors $\mathbf{a}_1$, $\mathbf{a}_2$, displaced relative to each other by the vector $\frac{1}{3}(\mathbf{a}_1 + \mathbf{a}_2)$. Owing to the translational symmetry, the Hamiltonian is diagonalized by a Fourier transform.

$$\hat{c}_a(\mathbf{r}) = \sum_{\mathbf{k}}^{\mathrm{BZ}} \hat{c}_a(\mathbf{k}) \frac{e^{i\mathbf{kr}}}{\sqrt{N}}, \qquad \hat{c}_a(\mathbf{k}) = \sum_{\mathbf{k}}^{\mathrm{SL}} \hat{c}_a(\mathbf{r}) \frac{e^{-i\mathbf{kr}}}{\sqrt{N}}, \tag{1.7}$$

where the summation over quasimomenta runs over the Brillouin zone (BZ), defined by the vectors dual to $\mathbf{a}_i$, while the summation in real space runs over the triangular sublattice (SL). Here N — is the number of unit cells.

$$\hat{H} = \sum_{\mathbf{k}}^{\mathrm{BZ}} \sum_{a,b} \hat{c}_a^+(\mathbf{k}) \mathcal{H}_{ab}(\mathbf{k}) \hat{c}_b(\mathbf{k}), \qquad \mathcal{H} = \begin{pmatrix} 0 & t\sum_{j=1}^3 e^{i\mathbf{k}\boldsymbol{\delta}_j} \\ t\sum_{j=1}^3 e^{-i\mathbf{k}\boldsymbol{\delta}_j} & 0 \end{pmatrix} \tag{1.8}$$

After the Fourier transform it remains to diagonalize the Hamiltonian in the sublattice index. Thus the elementary excitations in graphene are plane waves, into which states from the different sublattices enter with equal weights. The spectrum of excitations is shown in Fig. 1.1b.

$$\varepsilon(\mathbf{k}) = \pm\sqrt{t\left|\sum_{j=1}^3 e^{i\mathbf{k}\boldsymbol{\delta}_j}\right|} \tag{1.9}$$

The number of carbon atoms is $2N$; each atom is in a state of sp^3 hybridization and has one valence electron. Thus there are twice as many electrons as there are states in the Brillouin zone. Taking into account the twofold spin degeneracy, this means that the lower branch of the spectrum is completely filled while the upper one is empty, and the Fermi level lies at $\varepsilon = 0$. Therefore the physics of electrons in graphene is determined by states close to the points where the spectrum vanishes, $\mathbf{K}$, $\mathbf{K}' = (\pm\frac{4\pi}{3\sqrt{3}a}, 0)$. In their vicinity the Hamiltonian takes the form of equations (1.5).

$$\mathcal{H}(\mathbf{K}+\mathbf{k}) \approx -\frac{3}{2}ta(\sigma_x k_x + \sigma_y k_y), \quad \mathcal{H}(\mathbf{K}'+\mathbf{k}) \approx \frac{3}{2}ta(\sigma_x k_x - \sigma_y k_y). \tag{1.10}$$

It is also known that taking into account the spin–orbit interaction leads to the appearance of a mass term (the opening of a gap) of order 10 μeV [5].

1.2 Weyl electrons in solids

I consider electrons in the periodic potential of a crystal lattice, neglecting the electron–electron interaction.[2]

$$\hat{H} = \sum_i \frac{\hat{p}_i^2}{2m} + U(\mathbf{r_i} - \mathbf{a}), \qquad U(\mathbf{r}) = \sum_{\mathbf{a}} U_0(\mathbf{r} - \mathbf{a}) = U(\mathbf{r} + \mathbf{a}). \tag{1.11}$$

As is well known [6, §55], it is diagonalized by the Bloch wave functions $\psi_{\mathbf{k},n} = e^{i\mathbf{kr}} u_{\mathbf{k},n}(\mathbf{r})$, where $u_{\mathbf{k},n}(\mathbf{r} + \mathbf{a}) = u_{\mathbf{k},n}(\mathbf{r})$ is periodic on the lattice. Therefore the Hamiltonian is diagonal in the index $\mathbf{k}$, but may be non-diagonal in the band number n.

$$\hat{H} = \sum_{\mathbf{k}} \sum_{n,n'} \hat{c}^+_{\mathbf{k},n} \langle \psi_{\mathbf{k},n} | \hat{H} | \psi_{\mathbf{k},n'} \rangle \hat{c}_{\mathbf{k},n'}. \tag{1.12}$$

The physics of electrons in solids is governed by the bands lying near the chemical potential μ, and it is often sufficient to restrict oneself to only two bands — the valence band and the conduction band. Effectively, such an electron is described by a 2×2 Hamiltonian, which it is convenient to expand in the basis of the Pauli matrices.

$$\mathcal{H}(\mathbf{k}) = \Big(\langle \psi_{\mathbf{k},n} | \hat{H} | \psi_{\mathbf{k},n'} \rangle \Big)_{nn'} = \sum_{\mu=0}^{3} f_\mu(\mathbf{k}) \sigma^\mu. \tag{1.13}$$

Each of the functions f_μ is assumed to be analytic and can be expanded near some point of k–space according to $f_\mu(\mathbf{k}) = f_\mu(\mathbf{k}_0) + \hbar \mathbf{v}_\mu \cdot \delta\mathbf{k}$. If it happens that at some $\mathbf{k}_0$ the three functions f_i, $i = 1..3$ vanish, then this is precisely a Weyl point. One may expect that in the three-dimensional case such an accidental degeneracy occurs without any additional symmetry conditions, since there are three parameters $\mathbf{k}$ that can be varied [7].

The matrix v^ν_μ is transformed to bring the Hamiltonian to the form

$$\hat{H} = \hbar \mathbf{w} \mathbf{k} + \sum_i \hbar v_i k_i \sigma^i. \tag{1.14}$$

The first term leads to a tilt of the Dirac cone, which does not change the results of this work, and it will therefore be omitted below. [3] For simplicity I will also assume that the nodal velocities are isotropic, so that

$$\hat{H} = \chi \hbar v \boldsymbol{\sigma} \mathbf{k}, \tag{1.15}$$

where $\chi = \operatorname{sgn} \det(v^\alpha_\beta) = \pm 1$ — is the chirality of the node, and I take $v > 0$.

[2] The arguments presented here cannot, in general, be extended to a Hamiltonian with interaction, and the question of how to determine whether the band structure is preserved upon switching on the interaction remains open.

[3] This term plays a role in the calculation of photogalvanic effects in the presence of a magnetic field; when it is taken into account one speaks of type-II Weyl semimetals [8].

Magnetic monopoles

A tool for detecting Weyl points is the Berry connection [9], which, with the quasimomentum $\mathbf{k}$ chosen as the parameter, is defined according to

$$\mathbf{A}_n = i \langle n(\mathbf{k}) | \nabla_{\mathbf{k}} | n(\mathbf{k}) \rangle , \qquad A_n = \mathbf{A}_n \cdot d\mathbf{k}, \tag{1.16}$$

where $|n\rangle$ — is one of the eigenstates of the Hamiltonian (1.14). I also define the field induction $\mathbf{B}$ and the density of field sources ρ according to

$$\mathbf{B}_n = \nabla_{\mathbf{k}} \times \mathbf{A}, \quad \rho_n(\mathbf{k}) = \frac{1}{2\pi} \nabla_{\mathbf{k}} \cdot \mathbf{B}, \tag{1.17}$$

It turns out that for the Weyl Hamiltonian the Berry curvature vector $\mathbf{B}$ corresponding to the ground state represents the field strength of a point charge of magnitude $\frac{\chi}{2}$. Let $\hat{H} = (\boldsymbol{\sigma} \cdot \hat{\mathbf{k}})$, and let the states $|\pm\rangle$ denote the upper and lower levels.

$$B_\mu^\pm = -\epsilon_{\mu\nu\rho} \operatorname{Im} \langle \partial_\nu \pm | \partial_\rho \pm \rangle = -\epsilon_{\mu\nu\rho} \operatorname{Im} \frac{\langle \pm | (\partial_\nu \hat{H}) | \mp \rangle \langle \mp | (\partial_\rho \hat{H}) | \pm \rangle}{|E_+ - E_-|^2} =$$
$$= -\frac{1}{2} \operatorname{Im} \frac{\langle \pm | \epsilon_{\mu\nu\rho} [\hat{\sigma}_\nu, \hat{\sigma}_\rho] | \pm \rangle}{|E_+ - E_-|^2} = - \operatorname{Im} \frac{2i \langle \pm | \hat{\sigma}_\mu | \pm \rangle}{|E_+ - E_-|^2} = \mp \frac{k_\mu}{2|\mathbf{k}|^3}. \tag{1.18}$$

Since $\chi = -1$ interchanges the levels, $\rho = \chi \delta(\mathbf{k})$. For this reason, in the jargon, Weyl points are called "magnetic monopoles".

From this one can draw conclusions about the location of Weyl points in the Brillouin zone. According to the definitions (1.16), (1.17), the monopole density is an even function of $\mathbf{k}$ if there is time-reversal (T) symmetry, and an odd function in the presence of parity (P) symmetry.

$$T: \quad \mathbf{A}_n(\mathbf{k}) = \mathbf{A}_{\overline{n}}(-\mathbf{k}) \qquad \mathbf{B}_n(\mathbf{k}) = -\mathbf{B}_{\overline{n}}(-\mathbf{k}) \qquad \rho_n(\mathbf{k}) = \rho_{\overline{n}}(-\mathbf{k}) \tag{1.19}$$
$$P: \quad \mathbf{A}_n(\mathbf{k}) = -\mathbf{A}_{\overline{n}}(-\mathbf{k}) \qquad \mathbf{B}_n(\mathbf{k}) = \mathbf{B}_{\overline{n}}(-\mathbf{k}) \qquad \rho_n(\mathbf{k}) = -\rho_{\overline{n}}(-\mathbf{k}), \tag{1.20}$$

where $\overline{n}$ denotes the conjugate state: $|\overline{n}\rangle = T|n\rangle$, or $|\overline{n}\rangle = P|n\rangle$. Thus, in a TP–invariant system there can be no Weyl points, and a physical realization of a Weyl semimetal should be sought among materials without parity symmetry.

Experimental observation

The search for Weyl semimetals in nature was crowned with success in 2015, when it was discovered that materials of the type TaAs, TaP, NbAs, NbP possess this property. In the work [10] tantalum arsenide TaAs is considered, and from first principles 12 pairs of Weyl points are found in the Brillouin zone, as singularity points of the Berry field.

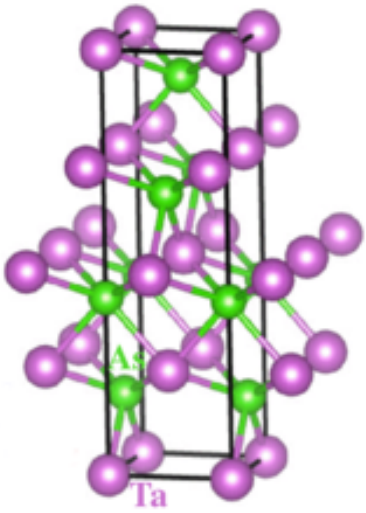

Figure 1.2: The TaAs lattice.

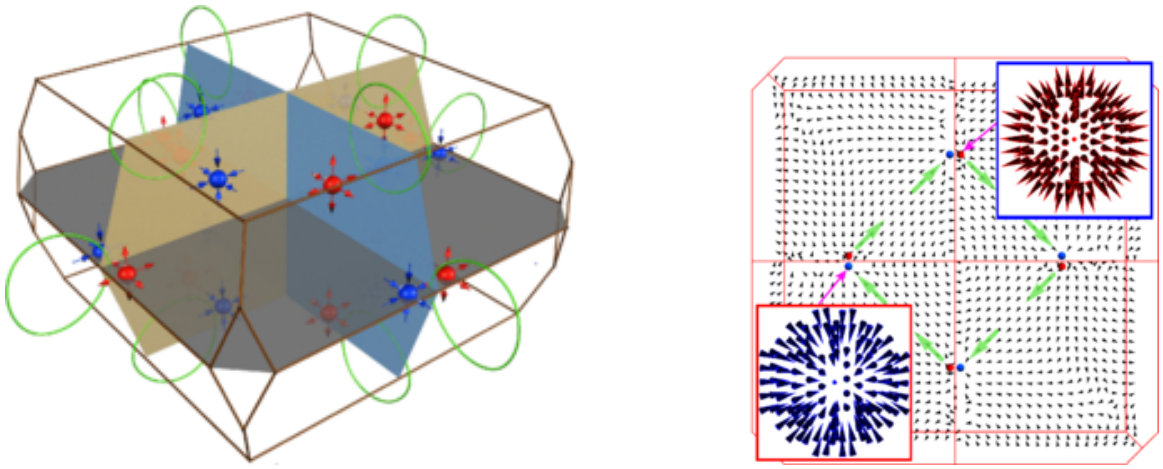

Figure 1.3: The Brillouin zone of TaAs and 12 pairs of Weyl monopoles. [10]
On the right the vector flux of the Berry field $\mathbf{B}$ is shown in the cross section $k_z = \text{const}$.

Approximately a year later, the experiment [11] was published, in which the Fermi surfaces in TaP were measured by the method of angle-resolved photoemission spectroscopy and a pair of Weyl nodes was discovered.

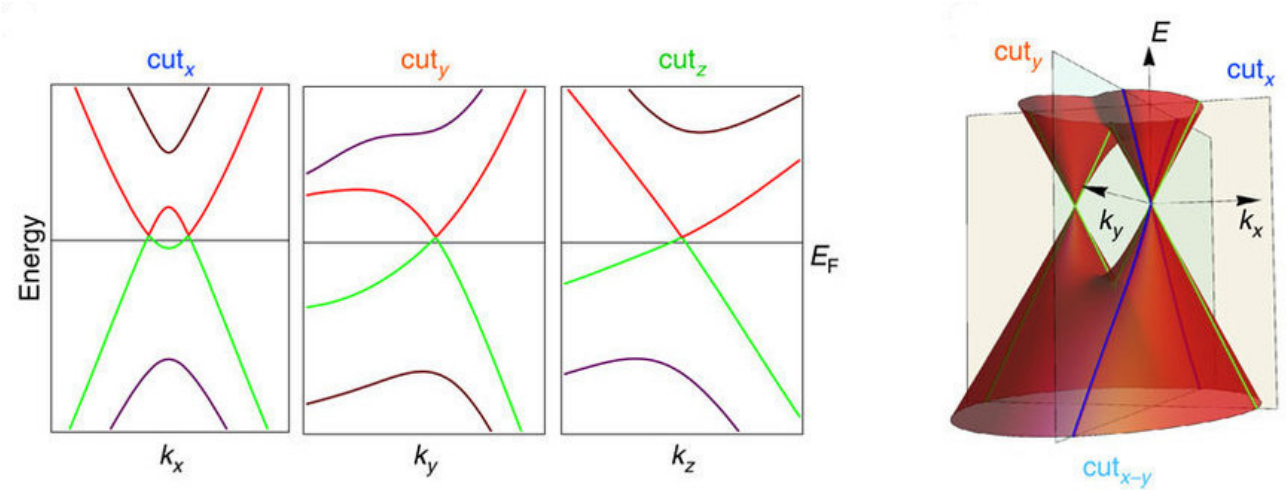

Figure 1.4: Numerical calculation of the band structure of TaP in the vicinity of a Weyl pair, confirmed by an experimental study. [11]

Topological protection

According to the Nielsen–Ninomiya theorem [12], regardless of the presence of symmetries, in any hopping model with non-interacting electrons the total chirality of all Weyl points equals zero. In other words, for every "monopole" there is an "antimonopole" somewhere in the Brillouin zone. This means that Weyl points are created and annihilate in pairs of opposite chirality. Since they can be located arbitrarily far apart, it follows that small changes in the Hamiltonian do not lead to the disappearance or appearance of Weyl monopoles.

Another consequence of the theorem is that in a T–symmetric Weyl semimetal the minimum possible number of monopoles is four, whereas in the P–symmetric case

there may be only two, since a pair can be created at the point $\mathbf{k} = 0$, which in the presence of T is forbidden by the property (1.19). The minimal models in which these cases are realized are considered below.

1.3 Toy models

The Delplace model

The simplest microscopic model describing Weyl semimetals that I am aware of is presented in [13].

Consider a hopping model on a cubic lattice (cube edge $a = 1$) with centered bases — two cubic sublattices (consisting of atoms of type A and type B), one shifted relative to the other by the vector $(\frac{1}{2}, \frac{1}{2}, 0)$. Accounting for hoppings to nearest neighbors (NN), next-nearest neighbors (NNN), as well as different intra-atomic energies $\varepsilon_{A,B} = \pm\Delta$ leads to the Hamiltonian

$$\begin{aligned} H = &\sum_{\mathbf{r}} \Delta(c_A^+(\mathbf{r})c_A(\mathbf{r}) - c_B^+(\mathbf{r})c_B(\mathbf{r})) + h.c. \\ &+ \sum_{\mathbf{r}} \sum_{n=0}^{3} t_n c_A^+(\mathbf{r})c_B(\mathbf{r} + \boldsymbol{\delta}_\mathbf{n}) + h.c. \\ &+ \sum_{\mathbf{r}} \sum_{n=0}^{3} t'_n c_A^+(\mathbf{r})c_A(\mathbf{r} + \boldsymbol{\epsilon}_\mathbf{n}) + h.c. \\ &+ \sum_{\mathbf{r}} \sum_{n=0}^{3} t_\perp (c_A^+(\mathbf{r})c_A(\mathbf{r} + \mathbf{e_z}) - c_B^+(\mathbf{r})c_B(\mathbf{r} + \mathbf{e_z})) + h.c., \end{aligned} \tag{1.21}$$

where $t_n = e^{in\pi/2}t$, $t'_n = e^{in\pi/2}t'$, $n = 0...3$, and t, t', $t_\perp$, Δ are assumed to be real. Such phases can be obtained if one imagines a magnetic field that possesses the symmetry of the lattice (and therefore the magnetic Brillouin zone coincides with the ordinary one) and threads the cell in the manner shown in 1.5.
The vectors $\boldsymbol{\delta}_n$ point from the center to the vertices of a square lying in the xy plane, whereas the $\boldsymbol{\epsilon}_n$ point along its sides.

$$\boldsymbol{\delta}_0 = \begin{pmatrix} \frac{1}{2} \\ -\frac{1}{2} \end{pmatrix} \quad \boldsymbol{\delta}_1 = \begin{pmatrix} \frac{1}{2} \\ \frac{1}{2} \end{pmatrix} \quad \boldsymbol{\delta}_2 = \begin{pmatrix} -\frac{1}{2} \\ \frac{1}{2} \end{pmatrix} \quad \boldsymbol{\delta}_3 = \begin{pmatrix} -\frac{1}{2} \\ -\frac{1}{2} \end{pmatrix} \tag{1.22}$$

$$\boldsymbol{\epsilon}_0 = \begin{pmatrix} 1 \\ 0 \end{pmatrix} \quad \boldsymbol{\epsilon}_1 = \begin{pmatrix} 0 \\ 1 \end{pmatrix} \quad \boldsymbol{\epsilon}_2 = \begin{pmatrix} -1 \\ 0 \end{pmatrix} \quad \boldsymbol{\epsilon}_3 = \begin{pmatrix} 0 \\ -1 \end{pmatrix} \tag{1.23}$$

The Fourier transform of $c_{A,B}(\mathbf{r})$ diagonalizes the Hamiltonian $H = \sum_\mathbf{k} c_a^+(\mathbf{k})H_{ab}(\mathbf{k})c_b(\mathbf{k})$.

$$H(\mathbf{k}) = 2t \sin k_+ \sigma_x + 2t \sin k_- \sigma_y + [\Delta - 2t'(\cos k_x + \cos k_y) + 2t_\perp \cos k_z]\, \sigma_z, \tag{1.24}$$

where we have denoted $k_\pm \equiv \frac{1}{2}(k_x \pm k_y)$. I also introduce the parameters $m_1 = \Delta/2t_\perp$, $m_2 = 2t'/t_\perp$. The spectrum has touching points at the coordinates $(k_x, k_y) = (0, 0)$

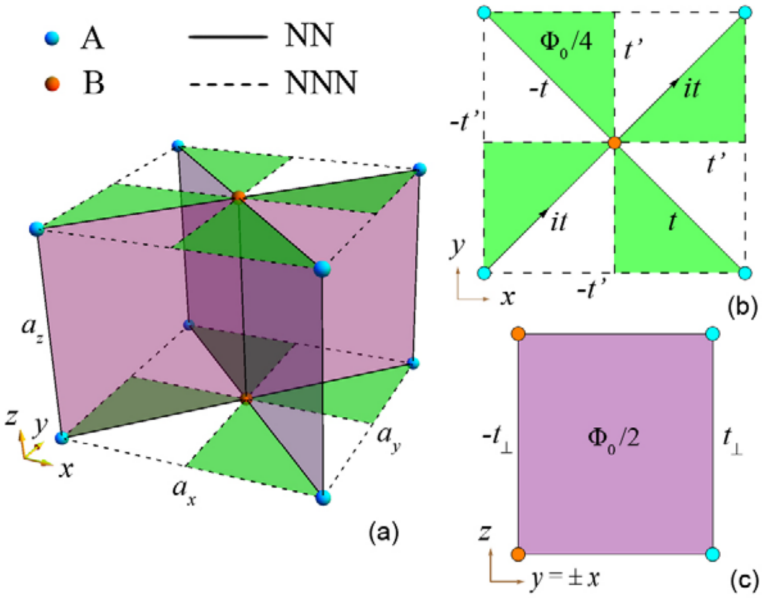

Figure 1.5: Crystal structure and definition of the hopping coefficients.

or (π, π) and $\cos k_z = -(m_1 - m_2 \cos k_+ \cos k_-)$. In the vicinity of these points the Hamiltonian has the long-wavelength expansion

$$H(\mathbf{k}) = 2tk_+\sigma_x + 2tk_-\sigma_y + 2t_\perp[m_1 - m_2 + 1 - k_z^2], \tag{1.25}$$

which I will use in the following in my work.

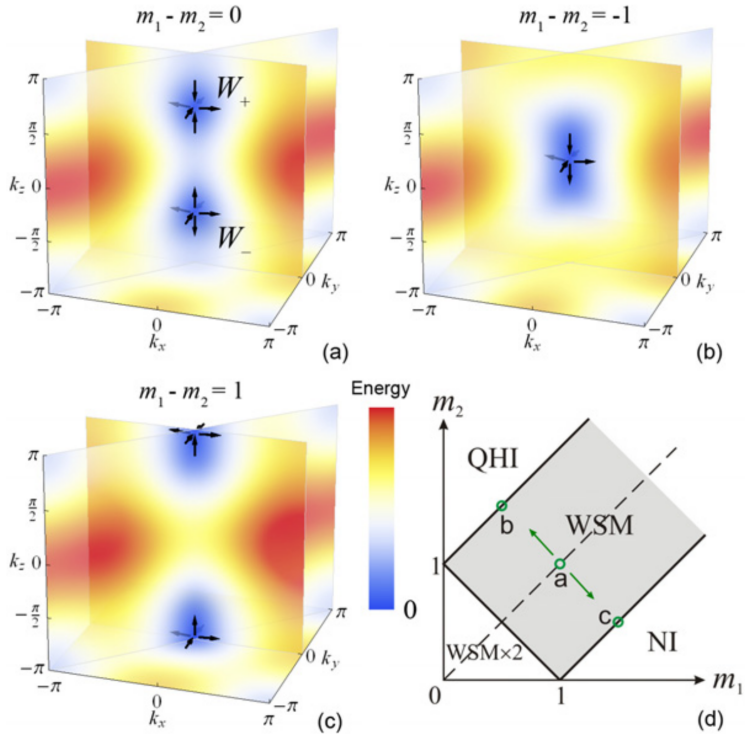

Figure 1.6: Position of the Weyl points for the values $m_1 - m_2 = 0, \pm 1$ and the phase diagram in the coordinates (m_1, m_2).

Chapter 2

Magnetoconductance

2.1 Statement of the problem

The problem consists in determining the conductance $G = dI/dV|_{V\to 0}$ in a ballistic $p{-}n$ junction based on a Weyl semimetal in the presence of a magnetic field.

Heterojunction

A heterojunction is a joining of semimetals doped with impurities of donor type n and acceptor type p. The effect of the impurities consists in raising/lowering the chemical potential, owing to the increase/decrease of the electron concentration. When semimetals of different types are joined, a redistribution of charge occurs — electrons flow from the n into the p region, which creates an electric potential $\varphi(z)$ that can be found self-consistently from the Poisson equation

$$\frac{d^2}{dz^2} e\varphi(z) = 4\pi e^2 \left[N(e\varphi(z)) + n_d(z) \right], \tag{2.1}$$

where $n_d(z) = \operatorname{sgn}(z)$ is the dopant concentration, approximated by a step function, and $N(\varepsilon) = \int_0^\varepsilon \nu(\epsilon) d\epsilon$ is the number of electrons in an undoped Weyl semimetal with energy less than ε (the charge distribution is computed against the background of the undoped semimetal). This problem was solved in [1], and it was found that the potential $\varphi(z)$ varies on the scale $\kappa^{-1} = \sqrt{\pi/4}(\hbar v)^{3/2}/|e|\Delta$, where Δ is the displacement of the node relative to the chemical potential. On this scale one can approximate the function $e\varphi(z) = -eEz$ as linear with coefficient $E \sim \Delta\kappa/|e| \sim \Delta^2/(\hbar v)^{3/2}$.

Ballistic regime

In solving the problem I will assume that the transport of the electron over the size of the $p{-}n$ junction potential κ^{-1} occurs without collisions with impurities, i. e. $\kappa^{-1} \ll l_{imp}$ — for this condition to hold, the impurity concentration must be sufficiently small. The impurity concentration is also assumed sufficiently small so that the appearance of impurity conduction bands need not be taken into account.

In the course of the solution it is assumed that the temperature $T = 0$. In effect this means that the conditions of applicability of the Landauer formula must be satisfied: the phase-breaking length $L_\varphi \propto 1/\sqrt{T}$ must be larger than the scale on which scattering occurs, κ^{-1}. One should also require that inelastic scattering processes

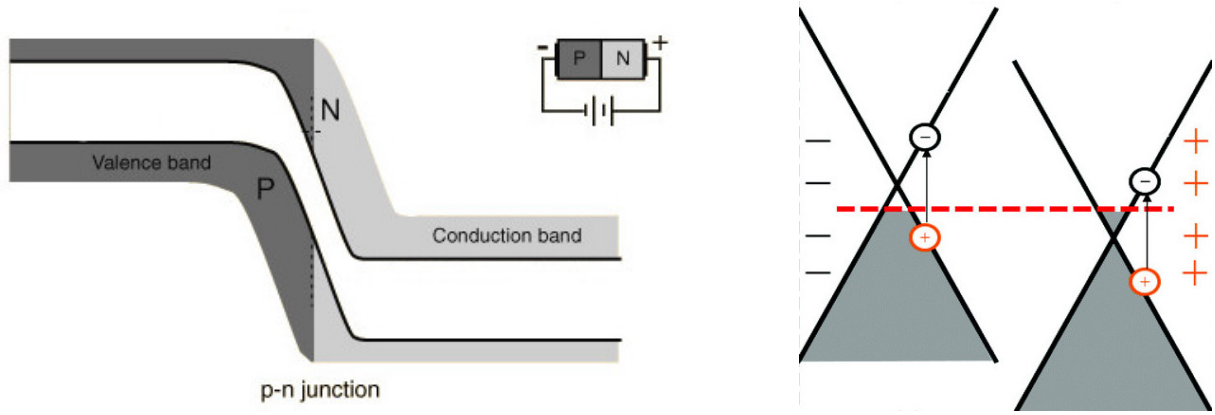

Figure 2.1: Heterojunction in a semiconductor and in a Dirac metal. The vertical axis shows the "total" energy $\varepsilon_{\mathbf{k}} + e\varphi$ — the electrochemical potential is constant in space.

contribute negligibly to the conductance; the electron–electron and electron–phonon interactions must be small, $l_{\text{e–e}}$, $l_{\text{e–ph}} \ll \kappa^{-1}$.

To take a finite temperature into account, one should also modify the Landauer formula (A.14)

$$\frac{e^2}{h}\sum_n T_n(\varepsilon = \mu) \quad \mapsto \quad \frac{e^2}{h}\sum_n \int d\varepsilon \left(-\frac{\partial n_F}{\partial \varepsilon}(\varepsilon)\right) T_n(\varepsilon). \tag{2.2}$$

and consider a $p{-}n$ junction of finite width, since in the linear-potential approximation the transmission coefficients do not depend on energy, $T \neq T(\varepsilon)$.

Plan of the solution

Below I will compute the conductance of the $p{-}n$ junction for different Hamiltonians. According to the Landauer formalism, whose description is given in appendix A, I will follow the standard plan.

0. Separate variables in the Schrödinger equation $\psi(\mathbf{r}) = \chi(x, y)\phi(z)$.
1. Solve the stationary Schrödinger problem $\hat{H}_\perp \chi_n = \varepsilon_n^\perp \chi_n$.
2. Solve the scattering problem $\hat{H}_\parallel(\varepsilon_n^\perp)\phi(z) = \varepsilon\phi(z)$.
3. Sum the transmission coefficients T_n over the transverse channels.

The scattering problem will always be solved at zero energy $\varepsilon = 0$, since in the linear potential $V(z) = -eEz$ an energy offset corresponds to a shift of the origin $V(z) - \varepsilon = -eE(z - z_0)$ and does not affect the answer.

Throughout this chapter, the notations for the electric and magnetic lengths will be used intensively (the electron charge $e < 0$).

$$l_E \equiv \sqrt{\frac{\hbar v}{|e|E}}, \qquad l_B \equiv \sqrt{\frac{\hbar c}{|e|B}}. \tag{2.3}$$

2.2 Conductance at zero field

The effective Hamiltonian describing a pair of Weyl nodes located at the points $k_x = \pm k_0$, together with the electric field induced by the $p{-}n$ junction, has the following form.

$$\hat{H} = \frac{\hbar^2}{2m}\left(\hat{k}_x^2 - k_0^2\right)\sigma_x + \hbar v\left(\hat{k}_y\sigma_y + \hat{k}_z\sigma_z\right) - eEz, \tag{2.4}$$

It is convenient to introduce the dimensionless parameter $\zeta \equiv \frac{\hbar k_0}{mv}$, which characterizes the velocity anisotropy at the Weyl node. Then, in the limit $k_0 \to \infty$, $\zeta \to 1$, the Hamiltonian factorizes into two single-cone Hamiltonians.

$$(\hbar v)^{-1}\hat{H} = \frac{\zeta}{2k_0}\left(\hat{k}_x^2 - k_0^2\right)\sigma_x + \hat{k}_y\sigma_y + \hat{k}_z\sigma_z + \frac{z}{l_E^2}, \qquad l_E^2 \equiv \frac{\hbar v}{|e|E}. \tag{2.5}$$

Scattering problem

In order to compute the conductance using the Landauer formula (A.14), one must solve the scattering problem, i.e. find the solution $\psi = e^{ik_x x + ik_y y}\phi(zl_E^{-1})$ of the equation

$$\left[\frac{\hbar l_E}{2mv}\left(k_x^2 - k_0^2\right)\sigma_x + k_y l_E\sigma_y + (-i\partial_z)\sigma_z + z\right]\phi(z) = \frac{\varepsilon}{\hbar v/l_E}\phi(z), \tag{2.6}$$

which at $z \to +\infty$ contains only a forward-propagating wave. The term involving the energy ε can be eliminated by shifting the z-coordinate, after which the equation takes the form

$$\begin{pmatrix} -i\partial_z + z & \Delta^* \\ \Delta & i\partial_z + z \end{pmatrix}\begin{pmatrix}\phi_1(z)\\ \phi_2(z)\end{pmatrix} = 0, \tag{2.7}$$

where $\Delta \equiv \frac{\hbar l_E}{2mv}\left(k_x^2 - k_0^2\right) + ik_y l_E$. To determine the transmission coefficient, I find the semiclassical wave function. The substitution

$$\phi_\pm^{1,2}(z) = \exp\left[\pm i\int k(z)dz\right]\varphi_\pm^{1,2}(z), \qquad k(z) \equiv \pm\sqrt{z^2 - |\Delta|^2} \tag{2.8}$$

and the expansion in the coefficient of the derivative ($\frac{d}{dz}\frac{1}{k(z)} \ll 1$) leads to

$$\varphi_\pm^{1,2}(z) = \frac{1}{\sqrt{k(z)}}\begin{pmatrix} c_\pm^1 \exp \mp\int\frac{dz}{2k(z)} \\ c_\pm^2 \exp \pm\int\frac{dz}{2k(z)}\end{pmatrix}. \tag{2.9}$$

At $z \to +\infty$ one should retain only the solution with positive probability current $j_\pm = \phi_\pm^+\hat{\sigma}_z\phi_\pm$, or, equivalently, positive group velocity $v_\pm(z) = \pm\partial k(z)/\partial z > 0$. The appropriate solution has the following asymptotics at $|z| \gg |\Delta|$.

$$\phi(z) = t\cdot\phi_-(z) \sim t\cdot\exp\left[-\frac{iz^2}{2} + \frac{i}{2}|\Delta|^2\ln\frac{2\sqrt{e}z}{|\Delta|}\right]\begin{pmatrix}1\\ -\frac{\Delta}{2z}\end{pmatrix}, \qquad z \to +\infty, \tag{2.10}$$

$$\phi(z) = \phi_+(z) + r\cdot\phi_-(z) \sim \exp\left[-\frac{iz^2}{2} + \frac{i}{2}|\Delta|^2 \ln\frac{2\sqrt{e}|z|}{|\Delta|}\right]\begin{pmatrix}1\\ -\frac{\Delta}{2z}\end{pmatrix} + \\ + r\cdot\exp\left[\frac{iz^2}{2} - \frac{i}{2}|\Delta|^2 \ln\frac{2\sqrt{e}|z|}{|\Delta|}\right]\begin{pmatrix}-\frac{\Delta^*}{2z}\\ 1\end{pmatrix}, \qquad z\to-\infty. \quad (2.11)$$

Comparing the asymptotic expansions (2.10) with (2.11), and using the fact that $\phi(z)$ is an entire function [14, §50], I find $t = \exp[-\frac{\pi}{2}|\Delta|^2]$. Since the probability current is given by the expression $j^z = v\phi^+\hat\sigma_z\phi$, the transmission coefficient is, as expected, $T = |t|^2$.

Landauer formula

Substitution into the Landauer formula yields

$$G(0) = \frac{e^2}{h}\int\frac{Sd^2k}{(2\pi)^2}\exp\left[-\pi\left(\frac{\hbar l_E}{2mv}\right)^2(k_x^2-k_0^2)^2 - \pi(k_y l_E)^2\right] \quad (2.12)$$

$$= \frac{2}{\zeta}\frac{e^2}{h}\frac{S}{(2\pi l_E)^2}\int_{-\infty}^{\infty}dx\,\exp\left[-\pi\frac{(x^2-x_0^2)^2}{x_0^2}\right] \quad (2.13)$$

where we have denoted $x_0 \equiv \frac{\zeta}{2}k_0 l_E = \frac{\hbar k_0^2 l_E}{2mv}$, and used the parameter $\zeta \equiv \frac{\hbar k_0}{mv}$.

$$G \simeq \frac{e^2}{h}\frac{S}{(2\pi l_E)^2}\cdot\begin{cases}\frac{\Gamma(\frac14)}{\sqrt{2}\pi^{\frac14}}\left[\frac{mv}{\hbar/l_E}\right]^{\frac12}, & \zeta k_0 l_E \ll 1\\ 2\zeta^{-1}, & \zeta k_0 l_E \gg 1\end{cases} \quad (2.14)$$

The numerical estimates below show that the condition $\zeta k_0 l_E \gg 1$ always holds; nevertheless, it is interesting to note the discovered influence of the cone coupling on the dependence of the conductance on the built-in electric field of the $p{-}n$ junction — $G \propto E^{\frac34}$, for $\zeta k_0 l_E \ll 1$.

2.3 Magnetoconductance

I will now find the conductance in the presence of a magnetic field $\mathbf{B}$, $\mathbf{A} = (-By, 0, 0)$, directed along the $p{-}n$ junction $B > 0$.

$$(\hbar v)^{-1}\hat H = \frac{\zeta}{2k_0}\left(\left(k_x - \frac{y}{l_B^2}\right)^2 - k_0^2\right)\sigma_x + \sigma_y\hat k_y + \sigma_z\hat k_z + \frac{z}{l_E^2}. \quad (2.15)$$

Here $l_E^2 \equiv \frac{\hbar v}{eE}$, $l_B^2 \equiv \frac{\hbar c}{eB}$ are the electric and magnetic lengths. I rescale the variables $y \mapsto l_B y$, $z \mapsto l_E z$, shift the argument $y \mapsto y + k_x l_B$, and separate the variables, in other words, I substitute the ansatz $\psi^{1,2}(x,y,z) = e^{ik_x x}\chi^{1,2}(yl_B^{-1} - k_x l_B)\phi^{1,2}(zl_E^{-1})$.

$$\left[\frac{\zeta}{2k_0 l_B}\left(y^2 - k_0^2 l_B^2\right)\sigma_x + \sigma_y\hat k_y + \frac{l_B}{l_E}\sigma_z\hat k_z + \frac{l_B}{l_E}z\right]\begin{pmatrix}\chi^1(y)\phi^1(z)\\ \chi^2(y)\phi^2(z)\end{pmatrix} = 0. \quad (2.16)$$

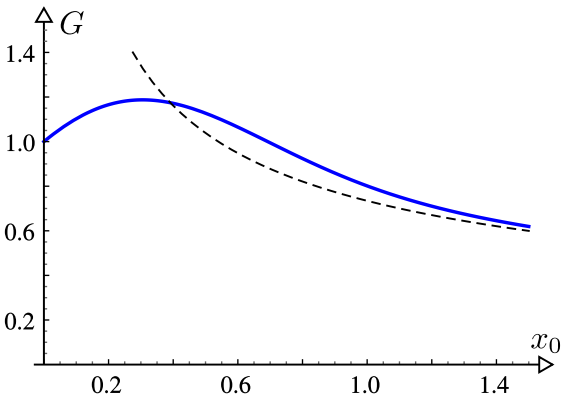

(a) $G(x_0)/G(k_0 = 0)$, $\zeta \equiv \frac{\hbar k_0}{mv}$.

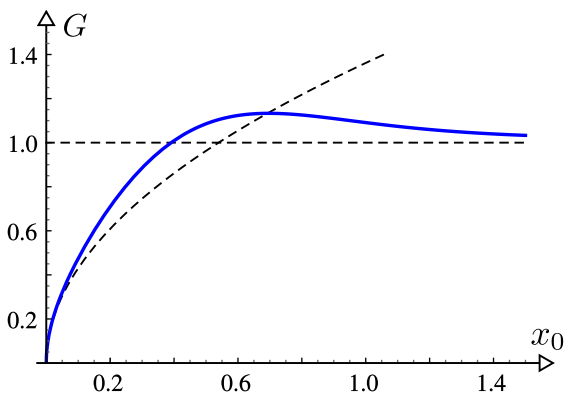

(b) $G(x_0)/G(k_0 = \infty)$, $\zeta = 1$.

Figure 2.2: Dependence $G(x_0)$, $x_0 = \frac{\zeta}{2} k_0 l_E$ compared with the asymptotics. Panel (a) shows the actual dependence $G(k_0^2)$ with the other parameters held constant. In panel (b) we set $\zeta = 1$, for comparison with the single-cone model; in reality $G \to \text{const} \neq 0$ as $k_0 \to 0$.

I denote $y_0 \equiv k_0 l_B$, so that the transverse equations read

$$\left[\frac{\zeta}{2y_0}\left(y^2 - y_0^2\right)\sigma_x + (-i\partial_y)\sigma_y\right]\chi_n(y) = \varepsilon_n \chi_n(y). \tag{2.17}$$

whereas the longitudinal equations have the same form as before

$$\left[(-i\partial_z)\sigma_z + (l_E/l_B)\varepsilon_n \sigma_x + z\right]\phi(z) = 0, \tag{2.18}$$

so the transmission coefficient equals $|t|^2 = \exp\left[-\pi \frac{l_E^2}{l_B^2}\varepsilon_n^2\right]$.

Transverse motion

Thus, the main problem is finding the eigenvalues ε_n^2.

$$\begin{pmatrix} 0 & \frac{\zeta}{2y_0}\left(y^2 - y_0^2\right) - \partial_y \\ \frac{\zeta}{2y_0}\left(y^2 - y_0^2\right) + \partial_y & 0 \end{pmatrix} \begin{pmatrix} \chi^1 \\ \chi^2 \end{pmatrix} = \varepsilon \begin{pmatrix} \chi^1 \\ \chi^2 \end{pmatrix} \tag{2.19}$$

At first glance, this Hamiltonian is supersymmetric [15], which means that the problem can be solved exactly. Unfortunately, the solution at $\varepsilon = 0$, which is so easily integrated, $\chi^{1,2}_{\varepsilon=0} = \exp \mp \frac{\zeta}{6y_0}(y^3 - 3y_0^2 y)$, is non-normalizable, and therefore one cannot construct a solution using the ladder operators $a^{\pm} = \frac{\zeta}{2y_0}(y^2 - y_0^2) \mp \partial_y$. One has to restrict oneself to finding corrections. I rescale $y \mapsto y/\sqrt{\zeta}$ and introduce $g \equiv (4\zeta y_0^2)^{-1}$ in order to leave a single parameter in the problem. The potential takes the form

$$\left[-\partial_y^2 + g\left(y^2 - \frac{1}{4g}\right)^2 - 2\sqrt{g}y\right]\chi = \frac{\varepsilon^2}{\zeta}\chi. \tag{2.20}$$

Clearly, one should build a perturbation theory in $\sqrt{g} \ll 1$; at $g = 0$ the potential splits into two harmonic oscillators. From the experience of studying the single-point model B, I know that the main contribution to the conductance comes from the zeroth Landau level. However, from the existence of the quasi-solution $\chi^{1,2}_{\varepsilon=0}$ it follows that the ground state satisfies $\varepsilon_0 > 0$, and it also follows that all corrections to it are absent in every order in $\sqrt{g}$. I will demonstrate this.

I move the origin of coordinates to the deep minimum $y_+ = y - \frac{1}{2\sqrt{g}}$, $\chi = \chi^1$.

$$\left[-\partial^2 + y_+^2(1+\sqrt{g}y_+)^2 - 1 - 2\sqrt{g}y_+\right]\chi = (\varepsilon^2/\zeta)\chi. \tag{2.21}$$

On the one hand, at $\varepsilon = 0$ the equation is formally satisfied by

$$\chi_{\varepsilon=0}(y) = e^{-\frac{y^2}{2} - \sqrt{g}\frac{y^3}{3}} = e^{-\frac{y^2}{2}} \sum_{n=0}^{\infty} \frac{(-)^n y^{3n}}{2^n n!} \sqrt{g}^n = \sum_{n=0}^{\infty} \chi^{(n)}_{\varepsilon=0}(y)\sqrt{g}^n. \tag{2.22}$$

On the other hand, according to perturbation theory, the first correction is found from the equation

$$\hat{H}^{(0)}\chi^{(1)} + \hat{H}^{(1)}\chi^{(0)} = \varepsilon^{(0)}\chi^{(1)} + \varepsilon^{(1)}\chi^{(0)}, \qquad \varepsilon^{(0)} = 0, \;\; \chi^{(0)} = e^{-\frac{y^2}{2}}. \tag{2.23}$$

Evidently it is solved by the (normalizable) functions $\chi^{(n)}_{\varepsilon=0}$, since $\hat{H}\chi_{\varepsilon=0} = 0$ holds in every order in the coupling constant $\sqrt{g}^n$.

It turns out that the correction to ε_0 is exponentially small in g and can be found using the instanton technique [16, (17)] or semiclassics; the latter method is described in detail in Appendix C. The answer is

$$\varepsilon_0^2 = \frac{\zeta}{\pi} \exp\left(-\frac{1}{3g}\right), \quad \frac{1}{g} = 4\zeta k_0^2 l_B^2. \tag{2.24}$$

Dependence of the conductance on the field

Using (2.24) and neglecting the shifts of the remaining levels, I sum the transmission coefficients in the limit $\zeta k_0^2 l_B^2 \gg 1$. I denote $B_0 \equiv \zeta \frac{\hbar c}{e} k_0^2$, $B_E \equiv \frac{cE}{v\zeta}$.

$$\begin{aligned} G(B) &= \frac{e^2}{h}\frac{S}{2\pi l_B^2} \sum_{\varepsilon_n} \exp\left[-\pi \frac{l_E^2}{l_B^2}\varepsilon_n^2\right] \\ &\approx \frac{e^2}{h}\frac{S}{2\pi l_B^2} \left\{ \exp\left[-\zeta \frac{l_E^2}{l_B^2} \exp\left(-\frac{4}{3}\zeta k_0^2 l_B^2\right)\right] + 2\sum_{n=1}^{n_{max}} \exp\left[-2\pi\zeta \frac{l_E^2}{l_B^2}(n + \delta n^{\pm})\right] \right\} \\ &\approx \pi G(0) \frac{B}{B_E} \left\{ \exp\left[-\frac{B}{B_E}\exp\left(-\frac{4}{3}\frac{B_0}{B}\right)\right] - 2 + \frac{2}{1 - \exp\left(-2\pi\frac{B}{B_E}\right)} \right\}. \end{aligned}$$

The function $G(B)$ has a maximum at $B = B_c$, which is completely determined by the first term and can therefore be estimated as

$$B_c \approx \frac{4}{3}\frac{B_0}{\ln \frac{4}{3}\frac{B_0}{B_E}}, \qquad \frac{B_0}{B_E} = (\zeta k_0 l_E)^2. \tag{2.25}$$

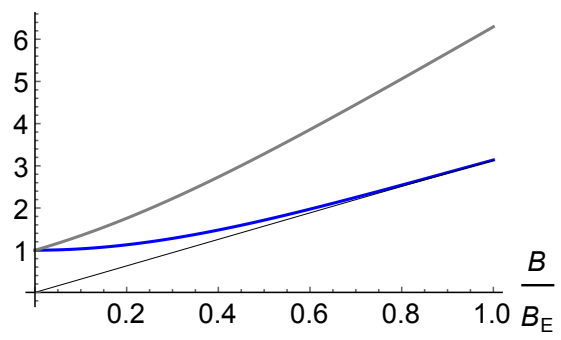

(a) $G(B)$ up to values $B < B_E \approx 4$ T.

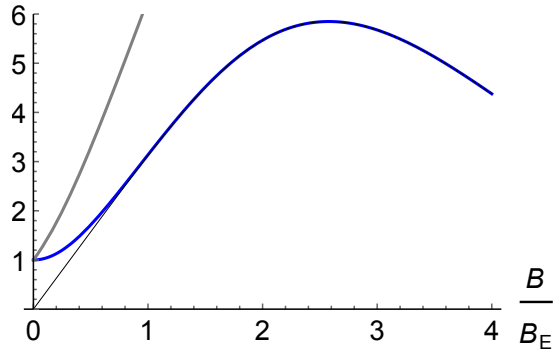

(b) $G(B)$ up to values $B < B_0 \approx 16$ T.

Figure 2.3: Magnetoconductance in the two-cone model compared with the single-cone model (gray) and the first term of the sum (black). For $B > B_0$ the results presented here are not applicable.

Numerical estimates

To understand the range of applicability of the obtained results, one needs to estimate the numerical values of the following parameters

$$\zeta \equiv \frac{\hbar k_0}{mv}, \quad l_E^2 \equiv \frac{\hbar v}{eE}, \quad l_B^2 \equiv \frac{\hbar c}{eB}, \qquad B_0 \equiv \zeta \frac{\hbar c}{e} k_0^2, \quad B_E \equiv \frac{c}{\zeta v} E. \tag{2.26}$$

The quantity $k_0 \simeq .02$ Å^{-1} for tantalum phosphide (TaP) according to the experiment [11], which is also consistent, in order of magnitude, with the numerical calculations [10]. In terms of the magnetic field this is $B_0 = \frac{\zeta}{\pi} \Phi_0 k_0^2 \simeq 26$ T.

From the data of [11] one can estimate $\zeta \simeq 1$, $v \simeq \alpha c$. According to the calculations [1], a fair estimate of the $p{-}n$ junction field is $E \simeq \Delta^2/(\hbar v)^{3/2}$, where Δ is the distance from the chemical potential to the Weyl node. According to [17], TaP has $\Delta \simeq 40$ meV, which corresponds to a "built-in" electric field $E \simeq 40$ V/m and an electric length $l_E \simeq 12$ Å, and hence the parameter $(\zeta k_0 l_E)^2 \simeq 4$.

These estimates show that $B_c < B_0$ and that the predicted extremum can indeed be observed in TaAs, TaP at fields on the order of several gauss.

2.4 Conclusion

In this work I have generalized and partially solved the problem of the magnetoconductance of a $p{-}n$ junction in a Weyl semimetal, treated in Ref. [1]. I have shown the relevance of describing such semimetals within the physically natural model [2] of a paired Weyl node, and identified a qualitatively new behaviour of the conductance $G(B)$ as a function of magnetic field. Namely, I found that, in contrast to the results of the single-cone model [1], in which the differential conductance has an anomalous positive sign at all fields, the two-cone model predicts a sign change of the differential

conductance at fields of order $\Phi_0 k_0^2$, which for the known semimetals of the TaAs, TaP type amounts to a few Tesla.

Appendix A

Landauer formalism

What is conductance?

The Landauer formula makes it possible to compute the conductance $G = dI/dV|_{V\to 0}$ of systems in which electric transport is governed by quantum effects [18].

Thus, according to the Landauer formula, in the simplest case the conductance of a perfectly transparent metal $T_n = 1$, at zero temperature $T = 0$, equals[1]

$$G = \frac{e^2}{h} N_\perp, \qquad N_\perp = \left\lfloor \frac{S k_F^2}{4\pi} \right\rfloor . \tag{A.1}$$

Here $N_\perp$ is the number of open channels (levels) of transverse motion, i. e. those participating in transport. It turns out that the dependence $G(S)$ has a step-like character at small S, while at large S it reaches the familiar regime $G \propto S$. Indeed, one is accustomed to considering that $G = \sigma \frac{S}{L}$, where σ is the conductivity. But according to the Landauer formula, the conductance does not depend on the length. The reason for such behavior lies in the assumption that the electrons move in the metal without interacting with each other or with defects in the metal. From this stems a limitation on the applicability of the Landauer formula — the electron motion can be considered "ballistic", i. e. collisionless, only for samples of length $L < L_\varphi$, where the so-called phase-breaking length $L_\phi \to \infty$ as $T \to 0$ [19, §5.5].

A.1 Statement of the problem

Suppose metallic wires with a voltage difference V are attached to the sample. From the electron's point of view, this means that to the left and to the right of the sample there are "reservoirs" with prescribed chemical potentials μ_1, $\mu_2 = \mu_1 - eV$. It is important to note that we are not speaking about the chemical potentials at the left and right edges of the sample, but precisely about the potentials of the attached wires, since the "wire–sample" contact itself also has a resistance. For more details, see the book [20, §5.2].

Transmission and reflection coefficients

Inside the sample the electron lives according to the laws of quantum mechanics; its motion is characterized by the probabilities of transmission T and reflection R of wave packets through the "scatterer", which are defined via the ratio of probability

[1] Here and below the formulas are given per single spin projection.

current densities. For the free-particle Hamiltonian, the Weyl Hamiltonian, and the two-node Hamiltonian, the current is expressed as

$$\hat{H} = \frac{\hat{p}^2}{2m} \quad \Rightarrow \quad \mathbf{j}(\mathbf{r}) = \frac{-i\hbar}{2m}\left(\psi^*\nabla\psi - \psi\nabla\psi^*\right), \tag{A.2}$$

$$\hat{H} = v(\boldsymbol{\sigma}\cdot\hat{\mathbf{p}}) \quad \Rightarrow \quad \mathbf{j}(\mathbf{r}) = v\psi^+\boldsymbol{\sigma}\psi, \tag{A.3}$$

$$\hat{H} = \frac{\hbar^2}{2m}(\hat{k}_z^2 - k_0^2)\sigma^z \quad \Rightarrow \quad j^z(\mathbf{r}) = \frac{-i\hbar}{2m}\left(\psi^+\sigma^z\partial_z\psi - (\partial_z\psi^+)\sigma^z\psi\right), \tag{A.4}$$

which follows directly from the evolution Schrödinger equation in the coordinate representation. However, it is more convenient to find the current density as the density of the mean value of the velocity

$$\mathbf{j}(\mathbf{r}) = \mathrm{Re}\,\psi^+(\mathbf{r})\hat{\mathbf{v}}\psi(\mathbf{r}) = \mathrm{Re}\,\psi^+\frac{i}{\hbar}[\hat{H},\mathbf{r}]\psi = \mathrm{Re}\,\psi^+\frac{\partial\hat{H}}{\partial\mathbf{p}}\psi. \tag{A.5}$$

Generally speaking, the transmission coefficients $T_{mn}(\varepsilon)$ depend on the initial channel n, the final channel m, and the electron energy ε.

In the case where the longitudinal variable z and the transverse variables x, y separate, the electron wave function factorizes as $\psi(\mathbf{r}) = \chi(x,y)\phi(z)$. Since the transverse motion is finite, the wave packet passes through the barrier while residing at some level of transverse quantization ε_n — a propagation channel. In this case the transmission coefficient from channel n to channel m is diagonal, $T_{mn} \propto \delta_{mn}$. When the variables do not separate, the notion of a channel is preserved, since at the edges of the sample, where the barrier potential varies weakly, the adiabatic approximation is appropriate.

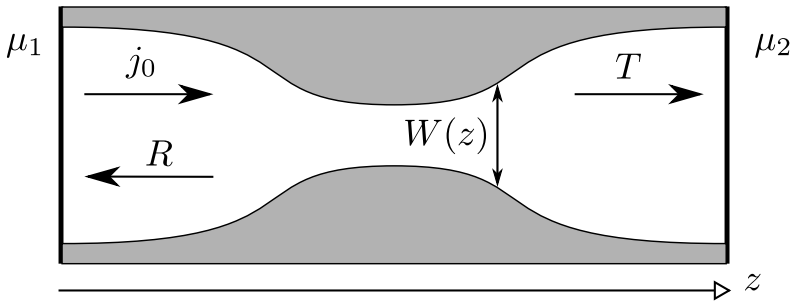

Figure A.1: Example of a quantum point contact.

Example

Suppose, for example, that I am dealing with a free particle of mass m, and the barrier is a narrowing cylindrically symmetric neck of radius $W(z)$; a longitudinal cross section of the contact is shown in Fig. A.1. Let $W(\mp\infty) = W_{1,2}$ at the edges. Then the transverse wave function and the energies on the left and on the right are

$$\chi(\boldsymbol{\rho}) = J_m\left(z_n^{(m)}\frac{\rho}{W_{1,2}}\right)e^{im\varphi}, \qquad \varepsilon_{m,n}^{\perp} = \frac{\hbar^2}{2m}\left(\frac{z_n^{(m)}}{W_{1,2}}\right)^2. \tag{A.6}$$

The indices m, n, which enumerate the n-th zero of the m-th Bessel function, also determine the channels of transverse quantization. If the radius of the constriction varies smoothly compared with the scale of the longitudinal motion, $W'(z)/W(z) \ll k_z$, i. e. for low-energy channels $\varepsilon^{\perp} \ll \varepsilon^{\parallel}$, one can approximately separate the variables and reduce the scattering problem to a one-dimensional one in an effective potential

$$\left[\frac{\hbar^2}{2m}\partial_z^2 + \varepsilon - \frac{\hbar^2}{2m}\left(\frac{z_n^{(m)}}{W(z)}\right)^2\right]\phi(z) = 0. \tag{A.7}$$

However, in this approximation the off-diagonal coefficients T_{nm} are absent.

Properties of the scattering coefficients

In sum, from the transport point of view, the scatterer S is completely characterized by the transmission and reflection coefficients T_{mn}, R_{mn} for incidence from the left, and T'_{mn}, R'_{mn} for incidence from the right.

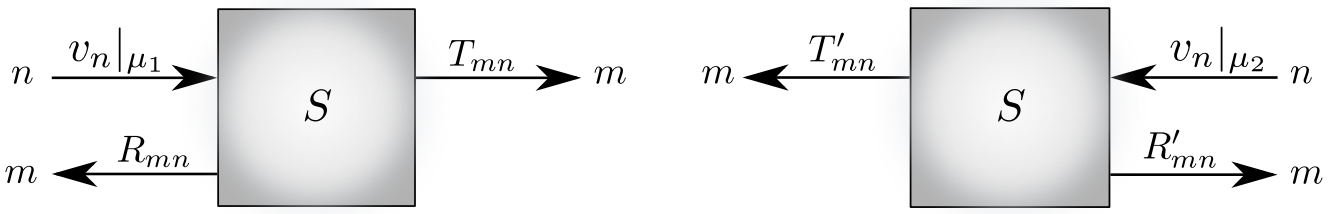

Figure A.2: Schematic representation of the transport properties of the sample.

Moreover, the following relation holds

$$T_m + R'_m = T'_m + R_m = 1, \qquad \text{where} \qquad T_n \equiv \sum_n T_{mn} \tag{A.8}$$

which means that all the flux arriving in channel m either tunneled through the scatterer or came from the same side after being reflected from the barrier. In the cases under consideration the potential is symmetric and $T = T'$, $R = R'$.

A.2 Derivation of the Landauer formula

Energy and velocity of electrons

Let me consider an electron with a prescribed energy $\varepsilon = \varepsilon_F + \xi$. This energy is distributed between the transverse and longitudinal motion. So, for example,

$$\xi_{\mathbf{k}_\perp, k_z} = \frac{\hbar^2}{2m}(k_\perp^2 + k_z^2 - k_F^2), \qquad \xi_{\mathbf{k}_\perp, k_z} = \pm\hbar v\sqrt{\mathbf{k}_\perp^2 + k_z^2} \tag{A.9}$$

for the free massive particle and the Weyl particle, respectively (the energy is measured from the Fermi level). It turns out that the value of the wave vector k_z is determined

by the channel number n, and only those channels are open for which $\varepsilon_{n,k} < \varepsilon$. There are $N_\perp = \left\lfloor Sk_F^2/4\pi \right\rfloor$ of them, and for each there exist two values of the wave vector $k_z > 0$ and $k_z < 0$ corresponding to a given energy — when computing the current one must choose those states that have the correct sign of the group velocity $v_{n,k} = \partial\xi_{n,k}/\partial k$.

In the cases under consideration the number of electrons moving to the right and to the left is the same, but this is not so, for example, for a single Weyl node in the presence of a magnetic field, owing to the existence of the chiral (zeroth) Landau level. Since the nodes exist in pairs of opposite chirality, the current will be nonzero only if the nodes are shifted in energy by $\Delta\mu$. The chiral current density is then given, according to the Landauer formula, by (B.8).

$$\Delta j = \frac{\Delta I}{S} = \frac{e^2}{h}\frac{\Delta\mu}{2\pi l_B^2} = \frac{e^3 B}{h^2 c}\Delta\mu. \tag{A.10}$$

For more details, read the article [21] or see the lecture [22].

Calculation of the current

When computing the current, I will also assume that an electron which has passed through the barrier, say, from the left reservoir, will always find a place in the right reservoir, i. e. I will not take into account the Pauli exclusion principle when determining the final state. For more details, see the book [20, §5.2].

The current through a transverse cross section, say, to the left (to the right it is the same) of the scatterer consists of three contributions (see Fig. A.2)

$$I = \int_0^\infty \frac{dk_z}{2\pi} \sum_{mn} e v_m(\varepsilon) \left[f_1(\varepsilon)\delta_{mn} - f_1(\varepsilon) R_{mn}(\varepsilon) - f_2(\varepsilon) T'_{mn}(\varepsilon) \right] \tag{A.11}$$

$$= /\varepsilon = \mu_1 + \xi/ = e \sum_{mn} \int \frac{d\xi}{h v_m(\xi)} v_m(\xi) T'_{mn}(\xi) \left[f_1(\xi) - f_2(\xi) \right] \tag{A.12}$$

$$= (\mu_1 - \mu_2) \cdot \frac{e^2}{h} \int d\xi \left(-\frac{\partial f}{\partial \xi} \right) \sum_{mn} T'_{mn}(\xi). \tag{A.13}$$

I note that the result does not depend on the dimensionality, since the summation over k_z is effectively one-dimensional and the density of states $\nu(\xi) = (2\pi\hbar(\partial\xi_{n,k}/\partial k))^{-1}$ cancels with the velocity $v_{n,k}$. Finally, the conductance is

$$G = \frac{e^2}{h} \int \frac{d\xi}{4T \operatorname{ch}^2 \frac{\xi}{T}} \sum_{mn} T_{mn}(\xi) \sim \frac{e^2}{h} \sum_{mn} T_{mn}(\varepsilon = \mu), \quad T \to 0. \tag{A.14}$$

The last formula can be rewritten as $G = \frac{e^2}{h} \operatorname{tr}(t^+ t)$, if one recalls that $T_{mn} = |t_{mn}|^2$ and assumes t_{mn} to be symmetric, which is not always true — in the general case, according to the Onsager relations, $t_{mn}(\mathbf{B}) = t_{nm}(-\mathbf{B})$.

Appendix B

Single-cone model

In this section I briefly reproduce the main results of the paper [1], following the solution plan described in Chapter 2.1.

B.1 Magnetic field along the heterojunction

Consider a $p{-}n$ junction in a Weyl semimetal in the presence of a magnetic field $\mathbf{B}$ aligned with the "built-in" electric field $\mathbf{E}$ of the $p{-}n$ junction.

$$\hat{H} = \hbar v \boldsymbol{\sigma} \cdot \left(\hat{\mathbf{k}} - \frac{e}{\hbar c} \mathbf{A} \right) - eEz, \tag{B.1}$$

In the gauge $\mathbf{A} = (-By, 0, 0)$ the momentum k_x commutes with the Hamiltonian.

$$(\hbar v)^{-1} \hat{H} = \sigma_x \left(k_x - \frac{y}{l_B^2} \right) + \sigma_y \hat{k}_y + \sigma_z \hat{k}_z + \frac{z}{l_E^2}, \qquad l_B^2 \equiv \frac{\hbar c}{|e|B}, \quad l_E^2 \equiv \frac{\hbar v}{|e|E}. \tag{B.2}$$

The substitution $\psi^{1,2}(\mathbf{r}) = e^{ik_x x} \chi^{1,2}(y l_B^{-1} - k_x l_B) \phi^{1,2}(z l_E^{-1})$ separates the variables.

$$\left[y\sigma_x + i\partial_y \sigma_y \right] \chi_n(y) = \varepsilon_n \chi_n(y), \tag{B.3}$$

$$\left[(l_E/l_B)\varepsilon_n \sigma_x + i\partial_z \sigma_z - z \right] \phi(z) = 0, \tag{B.4}$$

where in the last equation I set the energy to zero, since the transmission coefficient in a linear potential does not depend on it.

Transverse motion

The transverse equations (B.3) are easily solved and yield the Landau levels [14, §112].

$$(y \mp \partial_y) \chi^{1,2}(y) = \varepsilon \chi^{2,1}(y) \qquad \Rightarrow \qquad (-\partial_y^2 + y^2 - \varepsilon^2 \pm 1) \chi^{1,2}(y) = 0. \tag{B.5}$$

$$\chi_n = \begin{pmatrix} \psi_n^{\text{osc}} \\ \psi_{n+1}^{\text{osc}} \end{pmatrix} \quad \chi_0 = \begin{pmatrix} 0 \\ \psi_0^{\text{osc}} \end{pmatrix} \qquad \varepsilon_n = \sqrt{2n}, \;\; n \in \mathbb{N}_0. \tag{B.6}$$

Here $\psi_n^{\text{osc}}(y) \propto e^{-\frac{y^2}{2}} H_n(y)$ are the eigenfunctions of the harmonic oscillator.

Scattering problem

The longitudinal equations in the momentum representation take the form

$$i\partial_k \begin{pmatrix} \phi^1 \\ \phi^2 \end{pmatrix} = \begin{pmatrix} -k & \Delta_n \\ \Delta_n & k \end{pmatrix} \begin{pmatrix} \phi^1 \\ \phi^2 \end{pmatrix} \qquad \Delta_n \equiv \frac{l_E}{l_B}\varepsilon_n, \tag{B.7}$$

which coincides with the Landau–Zener equations, the momentum k playing the role of time. The probability of a transition to another level in the Landau–Zener problem is well known and equals $P = \phi^+\phi|_{k\to+\infty} = \exp(-\pi|\Delta_n|^2)$. Formally, this probability coincides with the transmission coefficient in the scattering problem $T = \phi^+\hat{\sigma}_z\phi$ — in both cases the initial wave functions were $\phi^1 = 1$, $\phi^2 = 0$.

Landauer formula

Summing the transmission coefficients $T_n = \exp(-2\pi\frac{l_E^2}{l_B^2}n)$ over the oscillator modes $n \in \mathbb{N}_0$, taking into account that each mode is degenerate $BS/2\Phi_0 = S/2\pi l_B^2$ times, gives the expression for the conductance

$$G = \frac{e^2}{h}\frac{S}{2\pi l_B^2}\sum_{n=0}^{\infty} T_n = \frac{e^3 BS/h^2 c}{1-\exp(2\pi\frac{vB}{cE})}. \tag{B.8}$$

In the limit $B \to 0$, I find

$$G(0) = \frac{e^2}{h}\frac{S}{2\pi l_E^2} = \frac{e^3 ES}{h^2 v}. \tag{B.9}$$

It is important to note here that the main contribution to the conductance comes from the zeroth Landau level, for which $T_0 = 1$; the contributions of the higher levels are exponentially smaller.

Appendix C

Homogeneous semiclassics

C.1 Tilted double-well potential

I will solve the stationary Schrödinger problem (the potential is shown in Fig. C.1)

$$\left[-\partial^2 + g\left(y^2 - \frac{1}{4g}\right)^2 - 2\sqrt{g}y\right]\chi(y) = 2\nu\chi(y). \tag{C.1}$$

to the first non-vanishing order in the parameter $g \ll 1$ using the method of uniform semiclassics. In terms of the variables $y_\pm = y \mp \frac{1}{2\sqrt{g}}$ the potential takes the form

$$\left[-\partial^2 + y_\pm^2(1 \pm \sqrt{g}y_\pm)^2 \mp 1 - 2\sqrt{g}y_\pm\right]\chi(y_\pm) = 2\nu\chi(y_\pm). \tag{C.2}$$

At $g = 0$ the problem splits into two harmonic oscillators.

$$\left[-\partial^2 + y_\pm^2 - (2\nu_\pm + 1)\right]\chi(y_\pm) \approx 0, \qquad |y_\pm| \ll 1/\sqrt{g}, \tag{C.3}$$

where the notation $\nu_+ = \nu$, $\nu_- = \nu - 1$ has been introduced. Each of the equations has eigenvalues $\nu_\pm = 0, 1, 2, \ldots$, and the original equation then has the spectrum $\nu = 0, 1^{(2)}, 2^{(2)}, \ldots$ The interaction $g \neq 0$, as is well known [14, §50], leads to exponentially small

$$\delta\nu_n \sim \text{const} \cdot \exp\left(-S_{\text{tunnel}}\right) = \text{const} \cdot g^{-n} \exp\left(-1/6g\right) \tag{C.4}$$

splittings of the degenerate levels, due to the tunneling overlap of the unperturbed wave functions, whose computation against a background of identical power-law shifts is usually of interest (in the potential under consideration the power-law corrections are absent, as a consequence of broken supersymmetry).

However, the method of [14, §50] gives an incorrect pre-exponential factor and, most importantly, is unable to determine the shift of the ground level ν_0, which plays the principal role in determining the conductance. It turns out that the correct first term of the asymptotic expansion can be obtained if, near the minima, one solves (C.3) exactly and matches the solutions with the global semiclassical solution

$$\chi(y) = C_+ \frac{\exp \int_0^y |k(z)|dz}{\sqrt{|k(y)|}} + C_- \frac{\exp - \int_0^y |k(z)|dz}{\sqrt{|k(y)|}}. \tag{C.5}$$

under the barrier $|y| < \frac{\text{const}}{\sqrt{g}}$, where the semiclassical momentum equals

$$|k(y)| = \sqrt{g\left(y^2 - \frac{1}{4g}\right)^2 - 2\sqrt{g}y - 2\nu}. \tag{C.6}$$

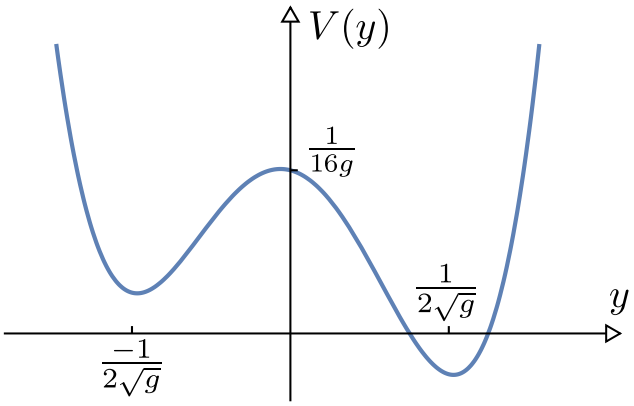

Figure C.1: Tilted supersymmetric double-well potential ($g = 2^{-6}$).

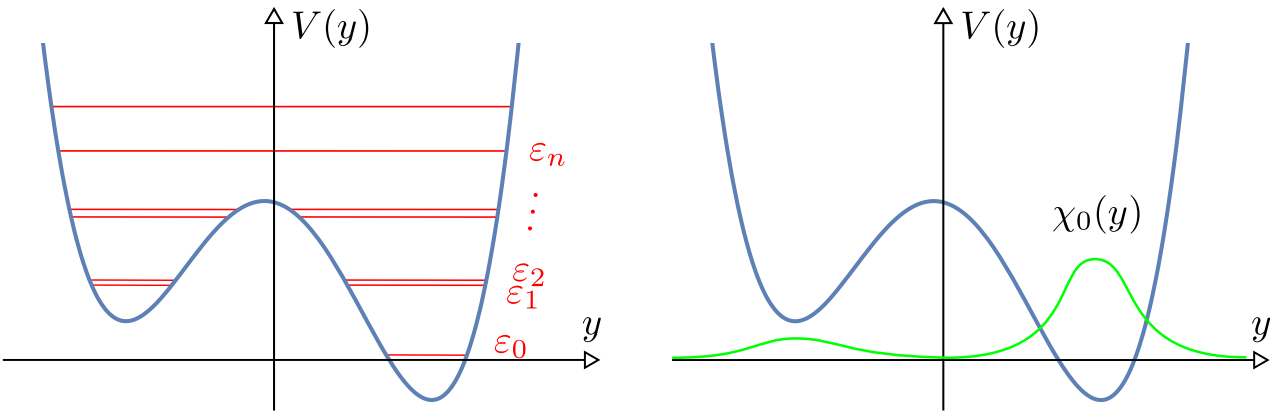

Figure C.2: Energy levels $\varepsilon_n = 2\nu_n$ and the ground-state wave function $\chi_0(y)$.

Matching of the semiclassical solutions

The solution that decays as $y \to +\infty$ is called the Hermite function $\psi_\nu^{\text{osc}}(y)$ and has the asymptotic behavior (the details are described in the following section)

$$\psi_\nu^{\text{osc}}(y) \sim \begin{cases} (2y)^\nu e^{-\frac{y^2}{2}}, & y \to +\infty \\ \cos\pi\nu(-2y)^\nu e^{-\frac{y^2}{2}} + \frac{\sqrt{\pi}}{\Gamma(-\nu)}(-y)^{-\nu-1}e^{\frac{y^2}{2}}, & y \to -\infty \end{cases} \tag{C.7}$$

It might seem that retaining the subleading term of the asymptotics is illegitimate against the background of the error in the leading contribution, but this is not so for the following reasons. First, I am interested in values of the argument $|y_\pm| \ll \frac{1}{\sqrt{g}}$, since the matching must take place in the region where (C.3) is still valid. Second, I am matching not values at a point, but functional dependences — expression (C.5) contains two exponentials with different signs, which means the asymptotics must have the same form. Third, the leading term contains the factor $\frac{1}{\Gamma(-\nu)} \to 0$ as $g \to 0$.

The semiclassical action near the turning points $|y| \sim \frac{\text{const}}{\sqrt{g}}$, i.e. at $|y_\pm| \ll \frac{1}{\sqrt{g}}$

$$S(y) = \frac{1}{8g}\int_0^{2\sqrt{g}y} \sqrt{(1-z^2)^2 - 16g(z+2\nu)}\, dz = \tag{C.8}$$

$$= \left[\frac{1}{8g}\left(z - \frac{z^3}{3}\right) + \frac{1}{2}\ln\left|1-z^2\right| + \nu \ln\left|\frac{1-z}{1+z}\right| + \mathcal{O}(g)\right]\Bigg|_0^{2gx} \tag{C.9}$$

$$= \frac{1}{12g} - \frac{y_+^2}{2} + \frac{1}{2}\ln\left[-4\sqrt{g}y_+\right] + \nu \ln\left[-\sqrt{g}y_+\right] + \mathcal{O}\left(y_+^3\right), \tag{C.10}$$

$$= -\frac{1}{12g} + \frac{y_-^2}{2} + \frac{1}{2}\ln\left[4\sqrt{g}y_+\right] - \nu \ln\left[\sqrt{g}y_-\right] + \mathcal{O}\left(y_-^3\right). \tag{C.11}$$

Comparison of (C.10) and (C.11) with expression (C.7) determines the quantization condition.

$$\frac{C_+}{C_-} = \frac{2^{\nu_+}\cos\pi\nu_+}{\sqrt{\pi}/\Gamma(-\nu_+)} \frac{e^{-\frac{1}{12g}-\nu\ln\left[\sqrt{g}\right]}}{e^{\frac{1}{12g}+\nu\ln\left[\sqrt{g}\right]}} = \frac{\sqrt{\pi}/\Gamma(-\nu_-)}{2^{\nu_-}\cos\pi\nu_-} \frac{e^{\frac{1}{12g}+\nu\ln\left[\sqrt{g}\right]}}{e^{-\frac{1}{12g}-\nu\ln\left[\sqrt{g}\right]}}. \tag{C.12}$$

I arrive at an equation for the energy ($\varepsilon = 2\nu$).

$$\left(\frac{g}{2}\right)^{2\nu} \Gamma(\nu)\Gamma(1+\nu)\,\mathrm{tg}^2\,\pi\nu = \frac{\pi}{2}e^{-\frac{1}{3g}}. \tag{C.13}$$

In the limit $g \ll 1$, when ν is close to an integer, so that $\nu_n = \lceil \frac{n}{2} \rceil + (-)^n \delta\nu_n$,

$$\delta\nu_0 = \frac{e^{-\frac{1}{3g}}}{2\pi}, \qquad \delta\nu_n = \sqrt{\frac{\lceil \frac{n}{2} \rceil}{2\pi}} \left(\frac{2}{g}\right)^{\lceil \frac{n}{2} \rceil} \frac{e^{-\frac{1}{6g}}}{\lceil \frac{n}{2} \rceil !}. \tag{C.14}$$

This is how the low-lying levels in the supersymmetric tilted double-well potential are described, and for $n > 0$ the stated formula gives splittings rather than shifts of the levels. The formula makes sense for $\lceil \frac{n}{2} \rceil < n_{\max} \approx \lfloor 1/32g \rfloor$. A numerical solution of the Schrödinger equation shows that the result $\delta\nu_0$ gives an answer with an error smaller than 3% all the way up to $g < \frac{1}{4}$, which is equivalent to $B < B_0$.

C.2 Hermite functions

The determination of the asymptotics of the Hermite functions $\psi_\nu(y)$ as $y \to -\infty$ deserves separate discussion. A suitable solution of (C.3) is easily found using Laplace's method.

$$\psi_\nu^{\text{osc}}(y) = e^{-y^2/2}\frac{\Gamma(\nu+1)}{2\pi i}\int_{-\infty}^{(0)} \frac{dt}{t^{\nu+1}} e^{2yt-t^2} \tag{C.15}$$

The function is normalized in such a way that when $\nu \in \mathbb{N}_0$ it reduces to the harmonic-oscillator wave function $\psi_n^{\text{osc}} = e^{-\frac{y^2}{2}} H_n(y)$. In the literature one also encounters the

parabolic cylinder function, in terms of which the Hermite function is expressed as $\psi_\nu^{\rm osc}(y) = \sqrt{2}^\nu D_\nu(\sqrt{2}y)$.

$$\psi_\nu^{\rm osc}(y \pm i0) \sim \begin{cases} (2y)^\nu e^{-\frac{y^2}{2}}, & y > 1 \\ e^{\mp i\pi\nu}(-2y)^\nu e^{-\frac{y^2}{2}} + \frac{\sqrt{\pi}}{\Gamma(-\nu)}(-y)^{-\nu-1} e^{\frac{y^2}{2}}, & y < -1 \end{cases} \tag{C.16}$$

References

[1] S. Li, A.V. Andreev, and B.Z. Spivak. Klein tunneling and magnetoresistance of $p-n$ junctions in Weyl semimetals. *Phys. Rev. B*, 94:081408, Aug 2016. arXiv:1605.02799.

[2] R. Okugawa and S. Murakami. Dispersion of Fermi arcs in Weyl semimetals and their evolutions to Dirac cones. *Phys. Rev. B*, 89:235315, Jun 2014. arXiv:1402.7145.

[3] В.Б. Берестецкий и Е.М. Лифшиц и Л.П. Питаевский. *Теоретическая физика. Том 4. Квантовая электродинамика.* ФИЗМАТЛИТ, Москва, 2006.

[4] A. Potter, I. Kimchi, and A. Vishwanath. Quantum oscillations from surface fermi arcs in weyl and dirac semimetals. *Nature Communications*, 5(5161), 2014. arXiv:1402.6342.

[5] S. Konschuh, M. Gmitra, and J. Fabian. Tight-binding theory of the spin-orbit coupling in graphene. *Phys. Rev. B*, 82:245412, Dec 2010. arXiv:1409.0388.

[6] Е.М. Лифшиц и Л.П. Питаевский. *Теоретическая физика. Том 9. Статистическая физика. Часть 2.* ФИЗМАТЛИТ, Москва, 2006.

[7] O. Vafek and A. Vishwanath. Dirac fermions in solids: from high-T_c cuprates and Graphene to topological insulators and Weyl semimetals. *Annual Reviews*, 5(83-112), 2014. arXiv:306.2272.

[8] S. Tchoumakov, M. Civelli, and M. Goerbig. Magnetic-field-induced relativistic properties in Type-I and Type-II Weyl semimetals. *Phys. Rev. Lett.*, 117:086402, Aug 2016. arXiv:1605.00994.

[9] Berry M.V. Quantal phase factors accompanying adiabatic changes. *Proceedings of the Royal Society of London A*, 392(1802), 1984. Michael's webpage.

[10] H. Weng, C. Fang, Z. Fang, A. Bernevig, and Xi Dai. Weyl semimetal phase in noncentrosymmetric transition-metal monophosphides. *Phys. Rev. X*, 5:011029, Mar 2015. arXiv:1501.00060.

[11] N. Xu et.al. Observation of Weyl nodes and Fermi arcs in tantalum phosphide. *Nature Communications*, 2016. arXiv:1507.03983.

[12] H.B. Nielsen and M. Ninomiya. The Adler-Bell-Jackiw anomaly and Weyl fermions in a crystal. *Physics Letters B*, 130(6):389 – 396, 1983.

[13] D. Delplace, J. Li, and D. Carpentier. Topological Weyl semi-metal from a lattice model. *ALJEFP*, 2012. arXiv:1202.3459.

[14] Л.Д. Ландау и Е.М. Лифшиц. *Теоретическая физика. Том 3. Квантовая механика. Нерелятивистская теория.* ФИЗМАТЛИТ, Москва, 2008.

[15] И.В. Криве и Л.Э. Генденштейн. Суперсимметрия в квантовой механике. *УФН*, 146(8):553–590, 8 1985.

[16] U.D. Jentschura and J. Zinn-Justin. Instantons in quantum mechanics and resurgent expansions. *Physics Letters B*, 596(1):138 – 144, 2004. arXiv:hep-ph/0405279.

[17] Su-Yang Xu et.al. Experimental discovery of a topological Weyl semimetal state in TaP. *Science Advances*, 1(10), 2015. arXiv:1508.03102.

[18] Г.Б. Лесовик и И.А. Садовский. Описание квантового электронного транспорта с помощью матриц рассеяния. *УФН*, 181(10):1041–1096, 2011. arXiv:1408.1966.

[19] Гантмахер, В.Ф. *Электроны в неупорядоченных средах.* ФИЗМАТЛИТ, 2013.

[20] Y. Imry. *Introduction to mesoscopic physics.* Oxford University Press, 1997.

[21] P. Baireuther, J.A. Hutasoit, J. Tworzydło, and C.W.J. Beenakker. Scattering theory of the chiral magnetic effect in a Weyl semimetal: interplay of bulk Weyl cones and surface Fermi arcs. *New Journal of Physics*, 18(4):045009, 2016. arXiv:1512.02144.

[22] C.W.J. Beenakker. Topological surface Fermi arcs in a Weyl semimetal and the chiral magnetic effect without Landau levels. *Tel Aviv University*, Jan 2016. YouTube.